Electronic Supplementary Material (ESI) for Inorganic Chemistry Frontiers.

Electronic Supporting Information

Ruthenium(II) Polypyridyl Complexes with π-Expansive Ligands: Synthesis and Cubosome Encapsulation for Photodynamic Therapy of Non-Melanoma Skin Cancer

Gina Elena Giacomazzo,[a†] Michele Schlich,[b†] Luca Casula,[b†] Luciano Galantini,[c,d] Alessandra Del Giudice,[c,d] Giangaetano Pietraperzia,[a,e] Chiara Sinico,[b] Francesca Cencetti,[f] Sara Pecchioli,[f] Barbara Valtancoli,[a] Luca Conti,[a*] Sergio Murgia,[b*] and Claudia Giorgi.[a*]

[a] Department of Chemistry "Ugo Schiff", University of Florence, Via della Lastruccia 3, 50019 Sesto Fiorentino (FI), Italy
[b] Department of Life and Environmental Sciences, University of Cagliari, 09124 Cagliari (CA), Italy
[c] Department of Chemistry, University of Rome La Sapienza, P.le A. Moro 5, 00185 Rome, Italy
[d] CSGI, Consorzio Interuniversitario per lo Sviluppo dei Sistemi a Grande Interfase, 50019, Sesto Fiorentino (FI), Italy
[e] European Laboratory for Non-Linear Spectroscopy (LENS), Via Nello Carrara 1, 50019, Sesto Fiorentino (FI), Italy
[f] Department of Experimental and Clinical Biomedical Sciences "Mario Serio", 50134, Florence, Italy

[†] These authors contributed equally to this work.

Emails for corresponding authors: *luca.conti@unifi.it*, *murgias@unica.it*, *claudia.giorgi@unifi.it*

Table of Contents

List of abbreviations

PDT = photodynamic therapy; RPCs = ruthenium(II) polypyridyl complexes; PSs = photosensitizer agents; PACT = photoactivated chemotherapy; ROS = reactive oxygen species; dppn = benzo[*i*]dipyrido[3,2-*a*:2′,3′-*c*]phenazine; dmbpy = 4,4′-dimethyl-2,2′-bipyridine; dcbpy = 2,2′-bipyridine-4,4′-carboxylic acid; $dcbpy^{2-}$ = 2,2′-bipyridine-4,4′-dicarboxylate; bpy = bipyridine, E-cubo = empty cubosomes; **Ru1**-**cubo** = **Ru1**-loaded cubosomes; **Ru2**-**cubo** = **Ru2**-loaded cubosomes; DCFH-DA = 2′,7′-dichlorodihydrofluorescein diacetate; DCF = 2′,7′-dichlorofluorescein.

1. Materials

All materials were of reagent grade and used without further purification unless otherwise specified.

Benzo[*i*]dipyrido[3,2-*a*:2′,3′-*c*]phenazine (dppn) was prepared through Schiff-base condensation reaction of 1,10-phenantroline-5,6-dione with 2,3-diaminonaphtalene, according to literature procedures.[1] The polymeric precursor $[Ru(CO)_2Cl_2]_n$, was obtained following the reaction of $RuCl_3 \cdot nH_2O$ with crystalline paraformaldehyde in formic acid 90% for 6 hours at reflux excluding light and isolated as a pale yellow powder through trituration from hexane.[2] The Ru(II)-intermediates *trans*-Cl[Ru**L**$(CO)_2Cl_2$] (**L** = dmbpy, dcbpy) were obtained through slight modifications of procedures reported in literature.[2,3] Briefly, $[Ru(CO)_2Cl_2]_n$ was added to hot solutions of dmbpy or dcbpy respectively in dry methanol or DMF, in 1:1.1 molar ratios. The reaction mixture was heated to reflux for 3 h under N_2 atmosphere and protected from ambient light. In the case of *trans*-Cl[Ru(dmbpy)$(CO)_2Cl_2$], the product was directly obtained following hot filtration from the reaction mixture whereas *trans*-Cl[Ru(dcbpy)$(CO)_2Cl_2$] was achieved upon evaporation of the solvent under vacuum and recrystallization from methanol: yields of 75 and 55% were respectively obtained for *trans*-Cl[Ru(dmbpy)$(CO)_2Cl_2$] and *trans*-Cl[Ru(dcbpy)$(CO)_2Cl_2$]. Ru(II) complexes **Ru1**-**2** are chiral and were isolated as a racemic mixture of Δ and Λ enantiomers. No attempts to obtain the pure enantiomers were made in this work.

Calf thymus DNA (*ct*-DNA) was purchased from Sigma Aldrich and dissolved in Tris-HCl buffer (10 mM Tris-HCl, 50 mM NaCl, pH 7.4). An absorbance ratio between 260 and 280 nm within 1.8-1.9:1 indicated that the biopolymer was sufficiently free of proteins.[4] A molar absorption coefficient at 260 nm of 6600 M^{-1} cm^{-1} was used to determine the *ct*-DNA concentration per nucleotide.[5]

Glycerol monooleate (MO, 1-monooleoylglycerol, RYLO MG 19 PHARMA, 98.1 wt%), for cubosomes preparation, was kindly provided by Danisco A/S (Denmark). Pluronic F108 (PF108, PEO132-PPO50-PEO132) was purchased from Sigma Aldrich. Fresh distilled water purified using a MilliQ system (Millipore) was used to prepare each sample and it was filtered with a 0.22 µm pore size hydrophilic filter prior to any use.

2. Synthesis and characterization of ruthenium(II) complexes

2.1. Synthesis of $[Ru(dmbpy)(dppn)_2](PF_6)_2$ (Ru1)$(PF_6)_2$

To a solution of *trans*-Cl[Ru(dmbpy)$Cl_2(CO)_2$] (80 mg, 0.19 mmol) in 8 mL of degassed 2-methoxyethanol were added dppn (129 mg, 0.39 mmol) and trimethylamine N-oxide (106 mg, 0.95 mmol). The reaction mixture was kept stirring for 4 h at reflux under nitrogen atmosphere. After cooling at r.t., addition of 3 mL solution 0.1 M of KPF_6 afforded the precipitation of the hexafluorophosphate salt of the ruthenium complex, which was filtered and then washed with water and chloroform. The crude product was purified by flash chromatography on silica gel (eluent: starting from DCM:MeOH 50:1 with 10% acetone to DCM:MeOH 30:1 with 10% acetone), affording **Ru1** as red powder. Yield 78%.

Anal. calcd for $C_{56}H_{36}F_{12}N_{10}P_2Ru$: C 54.24, N 11.30, H 2.93; found C 54.00, N 10.53, H 3.24, ^{1}H NMR (400 MHz, $(CD_3)_2CO$): δ 9.83 (d, $J_{c\text{-}b}$ = 8.0 H_z, 2H, H_c), 9.73 (d, $J_{c'\text{-}b'}$ = 8.0 H_z, 2H, $H_{c'}$), 9.23 (s, 2H, H_d), 9.20 (s, 2H, $H_{d'}$), 8.81 (s, 2H, H_5), 8.67 (d, J = 4.0 H_z, 2H, H_a), 8.62 (d, $J_{a\text{-}b}$ = 4.0, 2H, $H_{a'}$), 8.49-8.44 (m, 4H, H_e/$H_{e'}$), 8.18 (dd, $J_{b\text{-}c}$ = 8.0 Hz $J_{b\text{-}a}$ = 4.0 Hz, 2H, H_b), 8.12 (d, $J_{H2\text{-}H3}$ = 4.0 H_z, 2H, H_2), 7.95 (dd, $J_{b'\text{-}c'}$ = 8.0 H_z $J_{b'\text{-}a'}$ = 4.0 H_z, 2H, $H_{b'}$), 7.87-7.80 (m, 4H, H_f/$H_{f'}$), 7.38 (d, $J_{H3\text{-}H2}$ = 4.0 H_z, 2H, H_3), 2.61 (s, 6H, -CH_3) ppm. ^{13}C NMR (100 MHz, $(CD_3)_2CO$): δ 157.59, 155.08, 154.71, 152.34, 152.26, 152.13, 151.45, 141.51, 139.11, 135.80, 134.31, 134.23, 131.85, 131.77, 129.27, 129.19, 128.85, 128.80, 128.67, 128.45, 128.27, 125.89, 20.91 ppm. HR-MS (ESI+) m/z: calcd. for $C_{56}H_{36}N_{10}Ru^{2+}$ [**Ru1**]$^{2+}$ 475.10791; found 475.10791.

2.2. Synthesis of $[Ru(dcbpy^{2-})(dppn)_2]$ (Ru2)

To a solution of *trans*-Cl[Ru(dcbpy)$Cl_2(CO)_2$] (80 mg, 0.17 mmol) in 8 mL of degassed 2-methoxyethanol were added dppn (113 mg, 0.34 mmol) and trimethylamine N-oxide (95 mg, 0.85 mmol). The reaction mixture was stirred 6 h at reflux under N_2 atmosphere, the ruthenium complex precipitated from the reaction mixture after cooling at r.t. The crude product was collected, washed with water, and then triturated with $CHCl_3$ to afford **Ru2** as red powder, without the need of further purifications. Yield 50%.

Anal. calcd for $C_{56}H_{30}N_{10}O_4Ru$: C 66.73, N 13.90, H 3.00; found C 62.56, N 12.62, H 3.89, ^{1}H NMR (400 MHz, $(CD_3)_2SO$): δ 9.62 (d, $J_{c\text{-}b}$ = 8.0 H_z, 2H, H_c), 9.56 (d, $J_{c'\text{-}b'}$ = 8.0 H_z, 2H, $H_{c'}$), 9.27 (s, 2H, H_d), 9.22 (s, 2H, $H_{d'}$), 8.87 (s, 2H, H_5), 8.50 -8.40 (m, 2H, H_f and $H_{f'}$), 8.35 (d, $J_{a\text{-}b}$ = 8.0 $J_{a\text{-}b}$ = 4.8 H_z, 2H, H_a), 8.31 (d, $J_{a'\text{-}b'}$ = 4.8 2H, $H_{a'}$) 8.08 (dd, 2H, H_b), 7.93-7.84 (m, 4H, $H_{b'}$ and H_2), 7.82-7.75 (m, 4H, H_e and $H_{e'}$), 7.68 (d, J = 5.2 Hz, 2H, H3) ppm. HR-MS (ESI+) m/z: calcd. for $C_{56}H_{32}N_{10}O_4Ru^{2+}$ [**Ru2** + $2H^+$]$^{2+}$ 505.08188, found: 505.08177.

2.3. NMR, UV-Vis spectroscopy and fluorescence measurements

The ^{1}H, ^{13}C NMR, COSY and HSQC spectra were collected with a Bruker 400 MHz spectrometer. UV-Vis absorption spectra were acquired on a Perkin-Elmer Lambda 6 spectrophotometer. Fluorescence spectra and measurements of the phosphorescence signal of $^{1}O_2$ were carried out on a spectrofluorometer Horiba FluoroMax Plus.

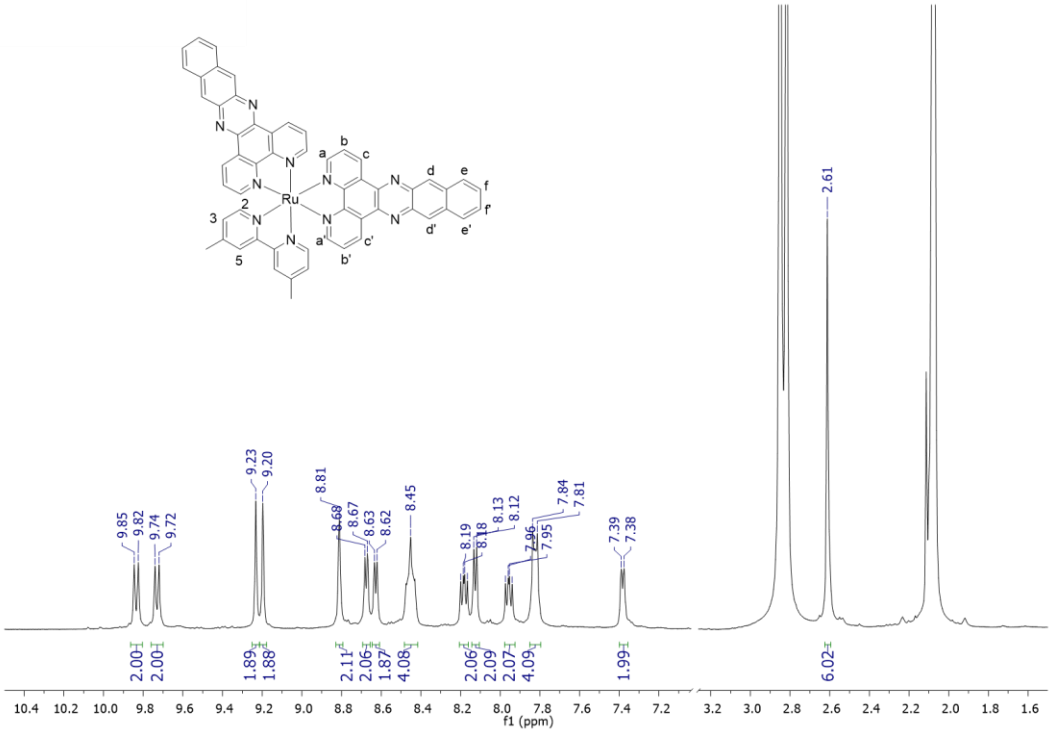

Fig. S1. ^{1}H NMR (400 MHz, $(CD_3)_2CO$) spectrum of complex **Ru1**.

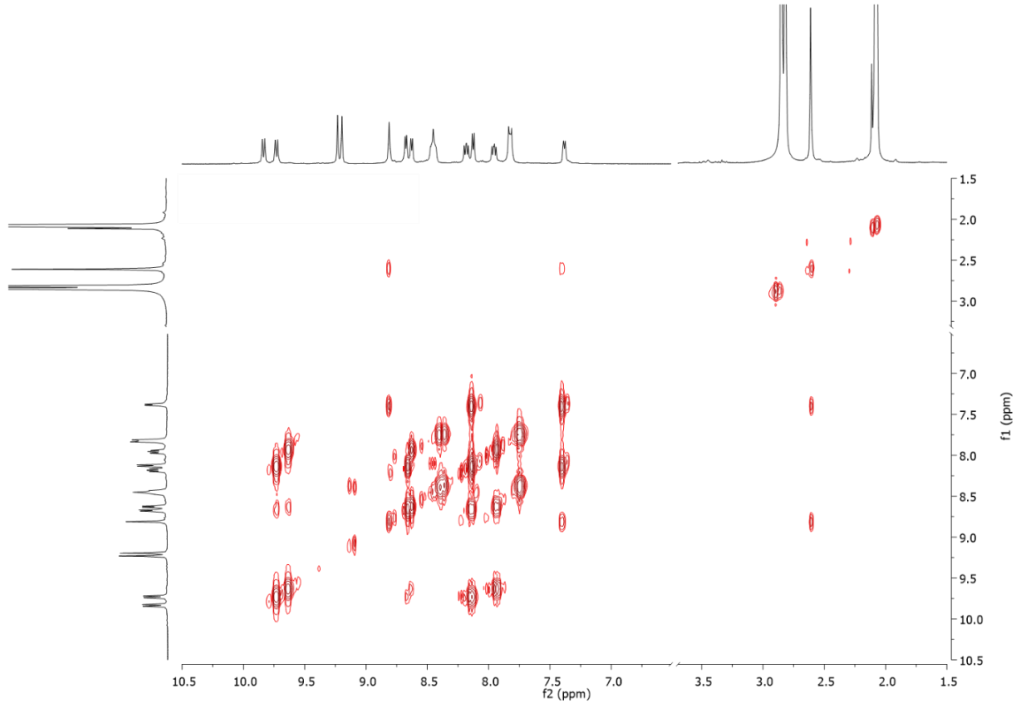

Fig. S2. $^{1}H^{1}H$ COSY spectrum of complex **Ru1** in $(CD_3)_2CO$.

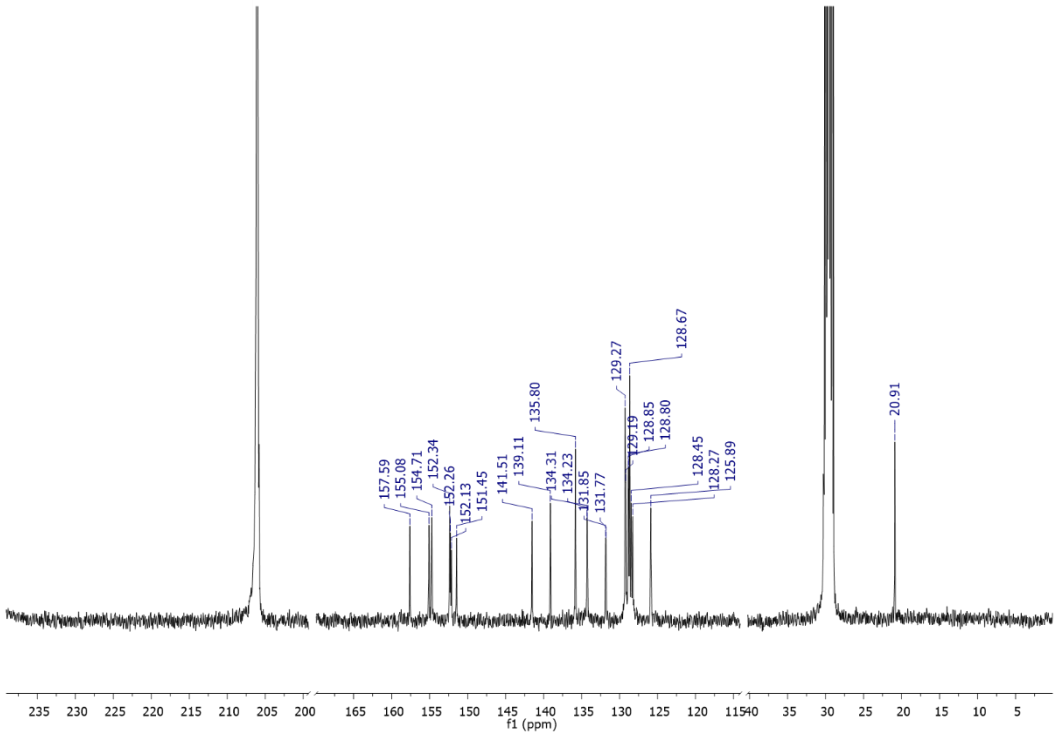

Fig. S3. ^{13}C NMR (100 MHz, $(CD_3)_2CO$) spectrum of complex **Ru1**.

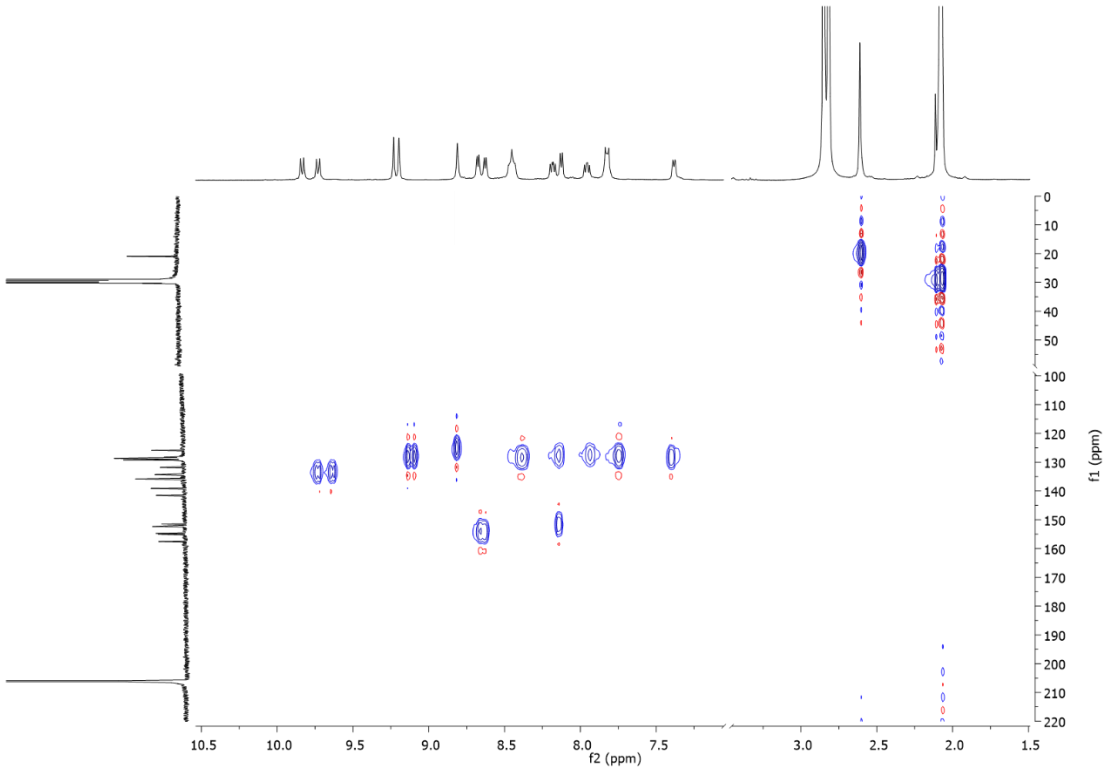

Fig. S4. HSQC spectrum of complex **Ru1** in $(CD_3)_2CO$.

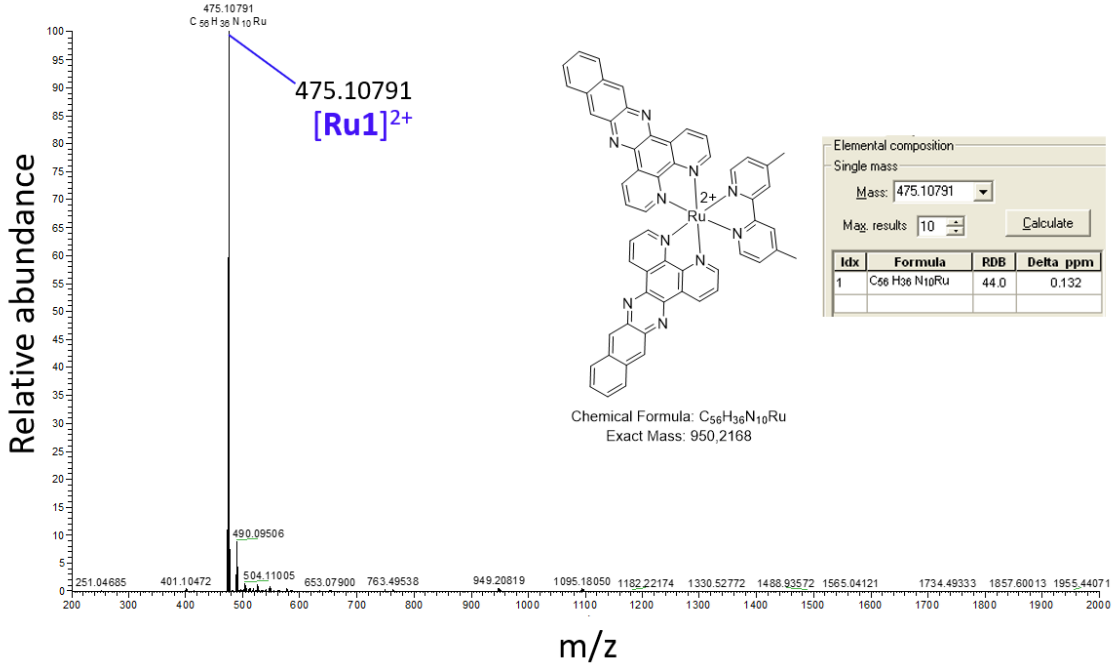

Fig. S5. HR-MS (ESI+) spectrum of ruthenium complex **Ru1** in acetonitrile.

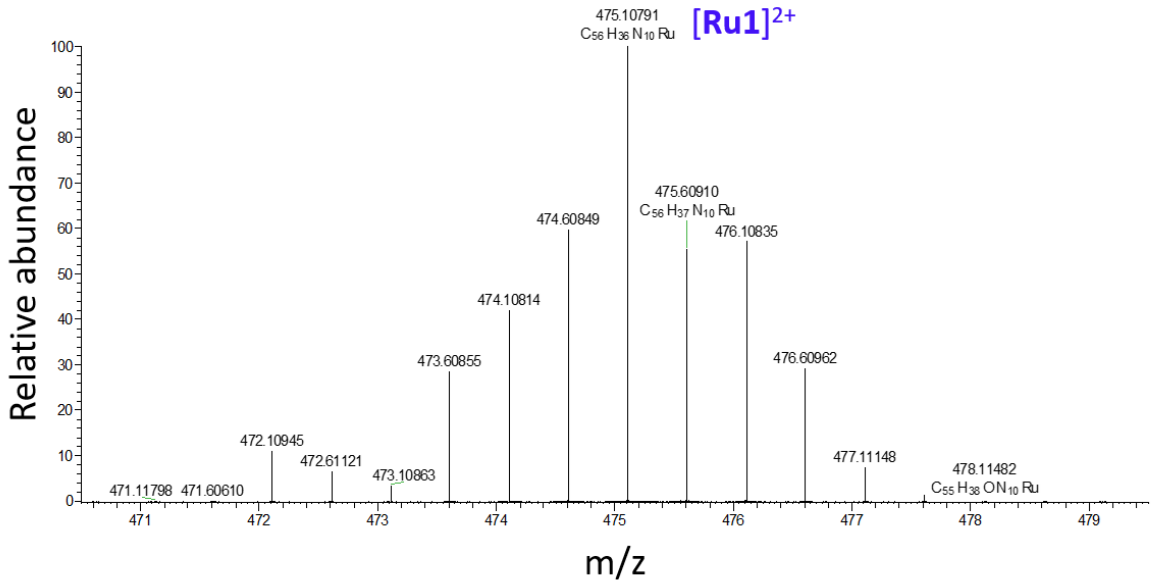

Fig. S6. Magnification of the measured isotopic pattern of the [**Ru1**]$^{2+}$ (z = 2) ion.

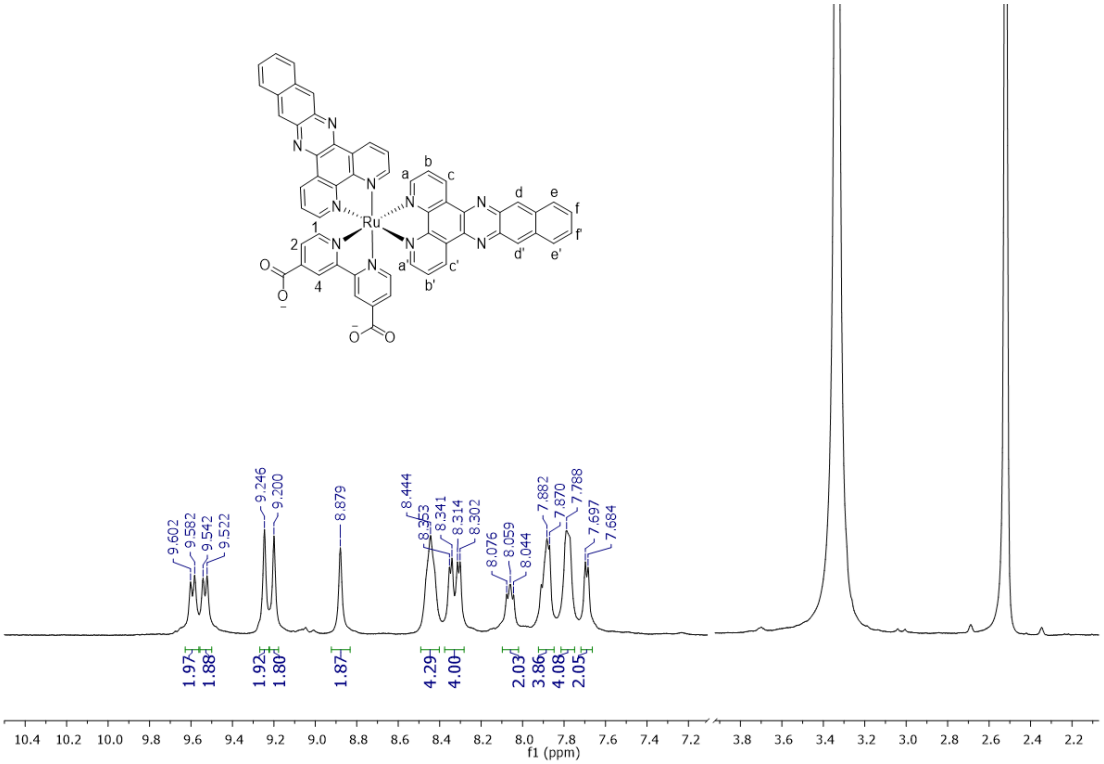

Fig. S7. ^{1}H NMR (400 MHz, $(CD_3)_2SO$) spectrum of complex **Ru2**.

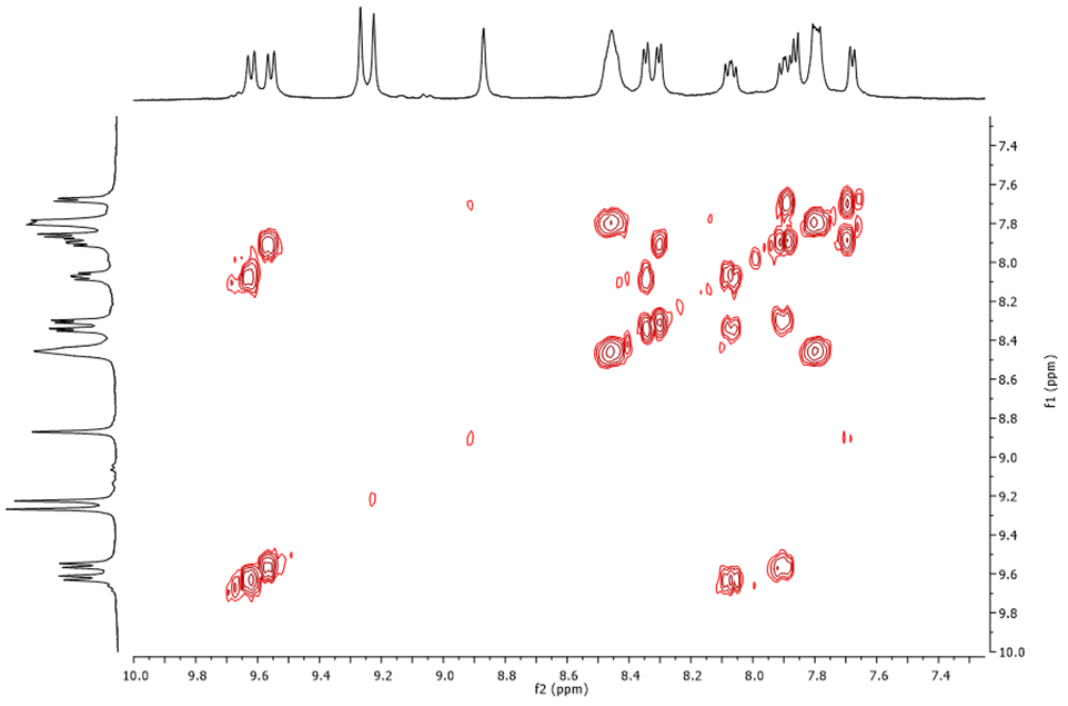

Fig. S8. $^{1}H^{1}H$ COSY spectrum of complex **Ru2** in $(CD_3)_2SO$.

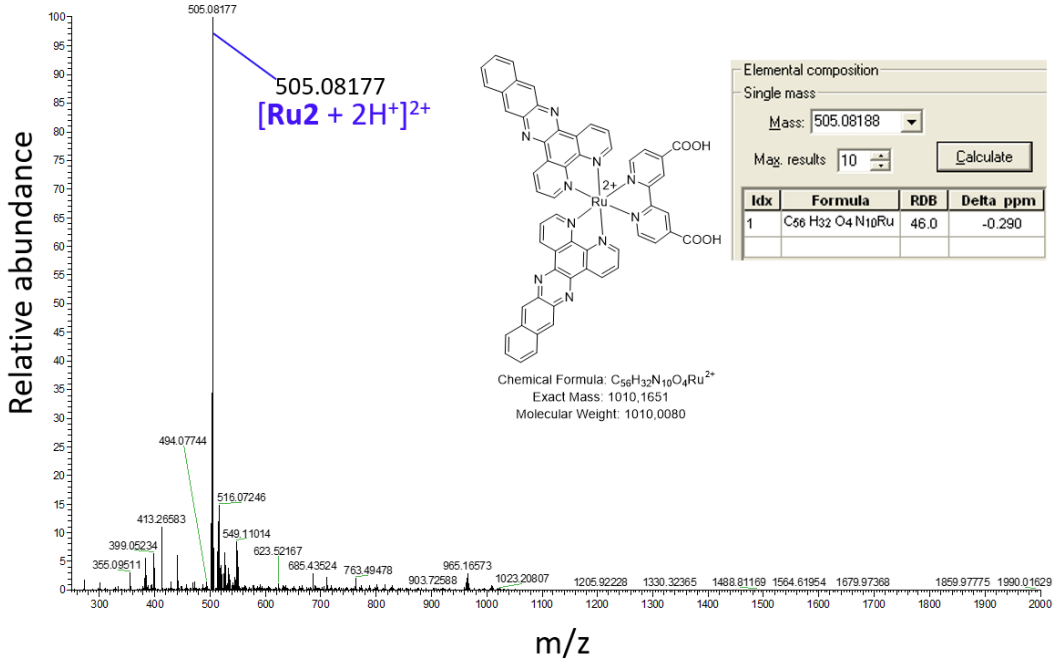

Fig. S9. HR-MS (ESI+) spectrum of ruthenium complex **Ru2** in acetonitrile.

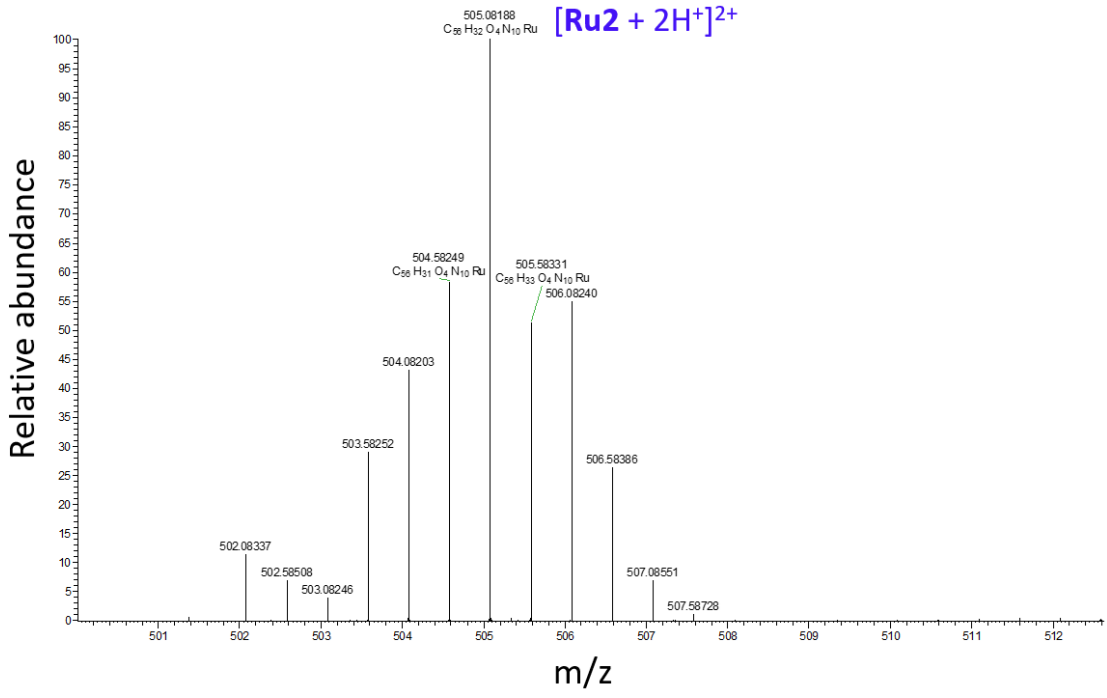

Fig. S10. Magnification of the measured isotopic pattern of the [**Ru2**+2H$^+$]$^{2+}$ (z = 2) ion.

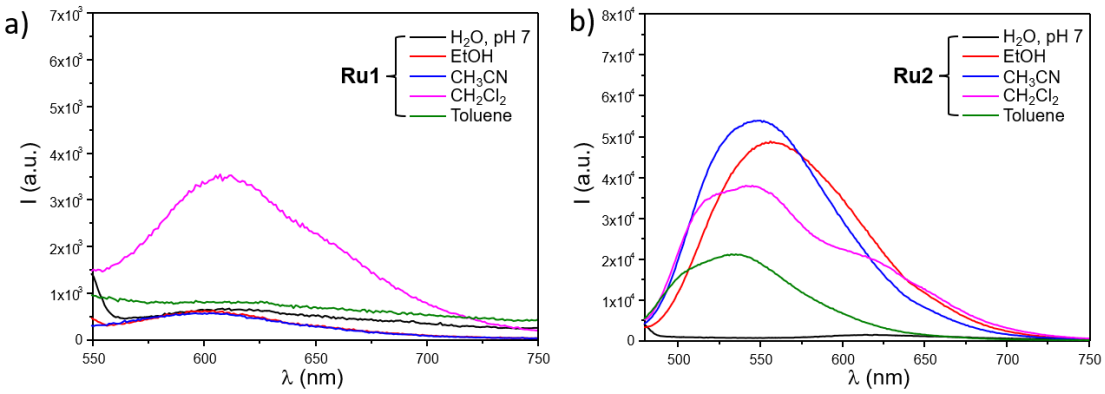

c)

Solvent	λ_{em} (**Ru1**)	λ_{em} (**Ru2**)
H_2O (pH 7)	-	615 nm
EtOH	-	557 nm
CH_3CN	-	547 nm
CH_2Cl_2	610 nm	545 nm
Toluene	-	535 nm

Fig. S11. Fluorescence emission of **Ru1** (a) and **Ru2** (b) in different solvents and maximum emission wavelengths (I_{em}) registered in the different media (c)([**Ru1**] = [**Ru2**] = 5 μM, λ_{exc} (**Ru1**) = 460 nm, I_{exc} (**Ru2**) = 410 nm).

2.4. Acid-base properties of Ru2

The acid-base properties of **Ru2** were investigated by monitoring the UV-Vis absorption and fluorescence spectra of aqueous solutions of the complex at different pH values. In the latter case, though the complex was poorly emissive in water, its residual fluorescence emission allowed to perform the fluorescence titrations. As shown in Figure S12a, the increase of pH of aqueous solutions of **Ru2** determined a progressive hypochromism at both the MLCT and IL absorption bands of the complex, with no significant blue or red shift observed in the range of pH investigated. On the other side, a significant enhancement of emission was observed with increasing the pH, accompanied by the presence of two inflection points, at *ca.* 2.5 and 4.5, suggesting a two-step acid-base equilibrium of the carboxylic moieties of the dcbpy ligand (Figure S12b-c). Analogously to what previously reported for parental dcbpy-containing RPCs,[6] only the second pKa value was determined. In particular, the pK_{a2} in the ground state ($pK_{a2}°$) was obtained from the UV-Vis absorption titration by fitting the data to the Henderson-Hasselbach equation:[7,8]

$$pH = pK_a° - log\frac{(A_i - A)}{(A - A_f)}$$

where A_i and A_f are respectively the initial and final absorbance values at 454 nm registered on increasing the pH of aqueous solutions of **Ru2**.

The pK_{a2} in the excited state (pK_{a2}*) was obtained from the fluorescence titration by using the following the equation:

$$pK_a^* = pH - log\frac{\tau}{\tau'}$$

where τ and τ' are respectively the excited state lifetimes of the protonated and deprotonated form of **Ru2**.[6]

From these measurements, values of 3.6 ± 0.3 and 4.6 ± 0.4 were respectively obtained for $pK_{a2}°$ and pK_{a2}* (see also Table 1 in the main text).

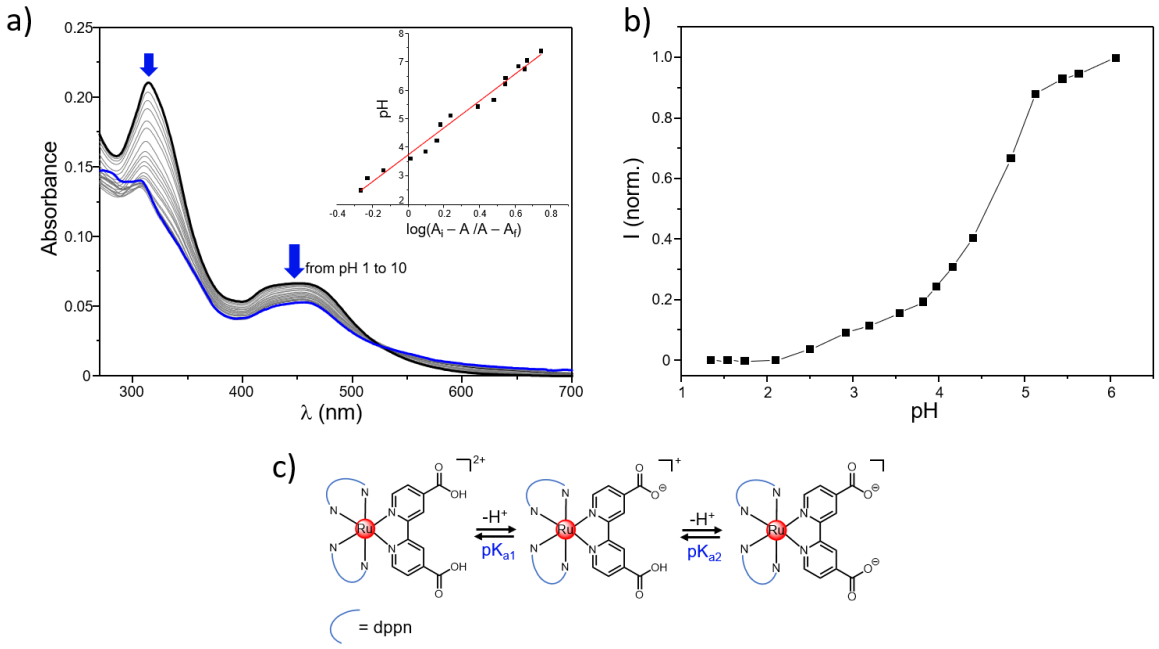

Fig. S12. Absorption spectra of **Ru2** (2 µM) in water collected at different pH and, in the inset, determination of the pH_{a2}° through the Henderson-Hasselbach-type equation (a). Fluorescence emission at 620 nm of **Ru2** (2 µM) in aqueous solution reported as a function of pH (λ_{exc} = 410 nm). Two-step acid-base equilibrium involving the carboxylic moieties of the dcbpy ligand of **Ru2** (c).

2.5. Singlet oxygen determination and DNA interaction

The singlet oxygen sensitizing properties of Ru(II) complexes were first analyzed spectrophotometrically, by using 1,5-dihydroxynaphthalene (DHN) as indirect $^1O_2$ reporter, accordingly to literature.[9] Briefly, air-saturated acetonitrile solutions containing DHN 3.3 x 10^{-4} M and RPCs 1 x 10^{-5} M were irradiated (LED emitting at 434 nm, 160 mW) in a quartz cuvette with 1 cm optical path over a total time of 200 s. Each spectrum was registered by using as blank reference a solution containing the selected compound at the same concentration of that of the measuring cuvette. The estimation of the relative rate constants for the DHN photooxidation processes (k_{obs}) was performed by applying the steady-state approximation to the $^1O_2$ intermediate, according to procedures previously described.[10] The quantum yields of $^1O_2$ generation (φ_Δ) by RPCs were determined through the direct measurement of $O_2(^1\Delta_g) \rightarrow {}^3O_2$ phosphorescence at 1270 nm, upon irradiation of compounds at 440 nm in air-saturated acetonitrile solutions. Experiments were run on solutions of RPCs at different concentrations, with the MLCT absorbance values within the range 0.08-0.2 and signals were collected by a N_2 cooled InGaAs photodiode. φ_Δ values were obtained as previously reported by comparison with $[Ru(phen)_3]^{2+}$, which was chosen as reference compound for $^1O_2$ production (φ_Δ = 0.38 ± 0.06).[11] Measurements were performed on a spectrophotofluorimeter Horiba FluoroMax.

The binding properties of ruthenium complexes towards *calf thymus* DNA (ct-DNA) were investigated spectrophotometrically, by adding increasing amounts of concentrated solutions of the biopolymer to aqueous solutions (TRIS buffer, pH 7.4) containing the tested RPC at fixed concentration (10 µM). The contribution arising from the absorbance of the DNA itself was eliminated by adding equal amounts of DNA both to the sample and to the reference solution. After each addition, samples were incubated for 10 minutes at 298.1 ± 0.1 K before collecting the absorption spectra. The intrinsic binding constants (K_b) with *ct*-DNA were determined accordingly to literature,[12,13] from the intercept-to-slope ratios of the plot of [*ct*-DNA]/$|\varepsilon_a-\varepsilon_f|$ *vs*. [*ct*-DNA] (see the inset of Figure 1d in the main text), where ε_a and ε_f correspond to $A_{obs.}$/[RPC] and to the molar extinction coefficient for the DNA-free metal compound. Linearity within the 0-3 µM range of [*ct*-DNA] was observed.

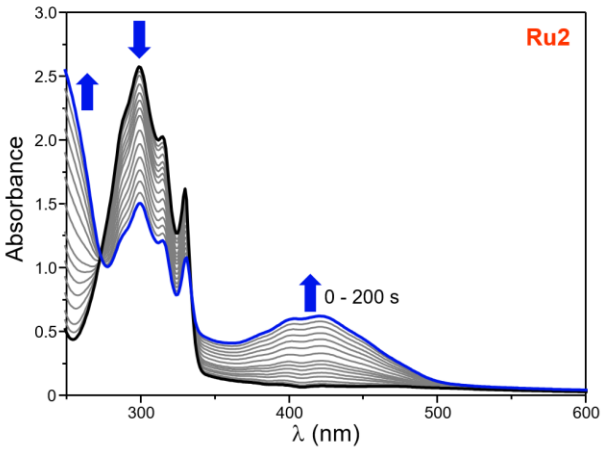

Fig. S13. Absorption spectra of acetonitrile solutions containing DHN and **Ru1** subjected to increasing irradiation times ([DHN] = 3.3 x 10^{-4} M, [**Ru1**] =10 µM, irradiation time 0-200 s).

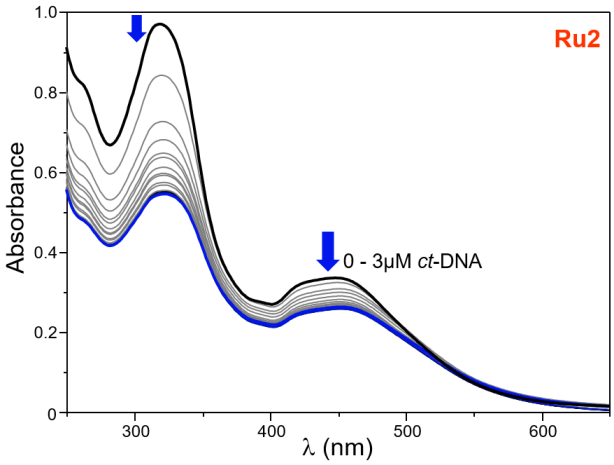

Fig. S14. Absorption spectra of aqueous solutions of **Ru2** registered in the presence of increasing concentrations of *ct*-DNA ([**Ru2**] = 10 µM, TRIS buffer pH 7.4).

3. Cytotoxicity and phototoxicity of free Ru1-2.

The human epidermoid carcinoma cell line A431 was purchased by ATCC and grown in DMEM (High Glucose) medium, supplemented with 10% fetal bovine serum, Penicillin/Streptomycin (50 units/mL each) and L-glutamine. Cells were cultured in 95% humidified atmosphere with 5% CO_2 at 37 °C.

A431 cells were seeded onto 96 well plates at a density of 10^4 cells/well. After 24h incubation, cells were treated with ruthenium complexes (**Ru1** or **Ru2**) solubilized in DMSO and diluted in complete medium (0.025-25 µM). Final concentration of DMSO was kept below 0.6% to avoid unspecific toxicity from the solvent. After 1 hour, the medium was replaced, and cells were either exposed to light (LED emitting at 462 nm, 18 mW/cm^2) for 30 minutes employing a customized cell illumination device (Figure S15) or incubated in the dark for the same time. Both groups were moved back to the incubator for further 24 hours before replacing the medium with 3-(4,5-dimethylthiazolyl)-2,5-diphenyltetrazolium bromide (MTT) (0.25 mg/ml) and incubated for 3 hours. The formazan crystals were dissolved in ethanol and optical density (OD) of wells was recorded on a plate reader (Infinite®

200 PRO, Tecan) at 570 nm. The optical density values were used to calculate the percentage of viable cells in each well, setting the OD of untreated cells (without PS and not exposed to light) as 100%. Each condition was tested in 5 replicates.

A customized cell illumination device (Figure S15a) was built using an array of 6 x 12 commercially available 5050 blue LED. The standoff distance between LED tops and the bottom of the culture plates was 1 cm. The emission spectrum of the device (Figure S15b) was measured using a USB4000 spectrometer (Ocean Optics).

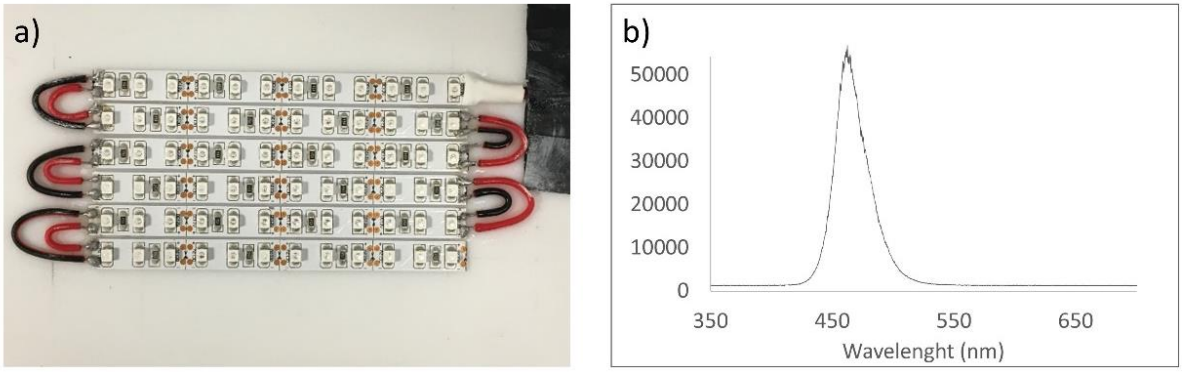

Figure S15. Picture of the customized cell illumination device, fabricated with an array of 12 x 6 5050 blue LED (a). Emission spectrum of the cell illumination device used for PDT experiments (λ_{max} = 462 nm) (b).

4. Hybrid Ru(II)-cubosome formulation: preparation, characterization, and *in vitro* evaluation of biological activity

4.1. Cubosomes preparation and characterization

Cubosomes were prepared by melting MO at 40 °C and dispersing ruthenium complexes (**Ru1** or **Ru2**) in the melted MO with the help of an ultrasonic bath. An appropriate amount of an aqueous solution of the stabilizers (PF108) was then added to the lipid phase and the mixture was ultrasonicated using a UP100H ultra- sonic processor developed by Hiescher (amplitude 90%; 1 s ON, 1 s OFF) for 5, 4, 3, 2, and 1 min cycles. The cubosome formulation investigated (**Ru1**-**cubo** and **Ru2**-**cubo**) had a composition of MO/PF108/ **Ru1** or **Ru2** = 3.3/0.3/0.02 % (w/w). Average hydrodynamic diameter (D) and polydispersity index (PDI, as a measure of the size distribution width) of the samples were determined by Dynamic Light Scattering (DLS) using a Zetasizer nano (Malvern Instrument, Worcestershire, United Kingdom). Samples were backscattered by a helium–neon laser (633 nm) at an angle of 173◦ and a constant temperature of 25 °C. Zeta potential was estimated using the Zetasizer nano by means of the M3-PALS (Phase Analysis Light Scattering) technique. To evaluate the drug entrapment efficiency, the complexes-loaded cubosomes were separated from the free complex by dialyzing the formulation using a tubing cellulose membrane (14 kDa molecular weight cutoff, Sigma Aldrich) against 2 L of water for 2 h (water was changed after 1 h) at room temperature. Drug quantitative determination was performed by UV-vis spectroscopy at 325 nm after cubosomes disruption in methanol, using a Synergy 4 multiplate reader (BioTek, Winooski, USA). The encapsulation/entrapment efficiency (EE%) was calculated exploiting the following expression:

$$EE\% = \frac{mass\ of\ drug\ after\ dialysis}{mass\ of\ weighted\ drug}\ x\ 100\%$$

4.2. Stability of the cubosomes dispersion

A medium-term stability study of the formulation stored at 25 °C was performed by monitoring mean hydrodynamic diameter, polydispersity index, and zeta potential for 30 days. The samples were visually inspected before every DLS measurement to check the absence of large aggregates or phase separation.

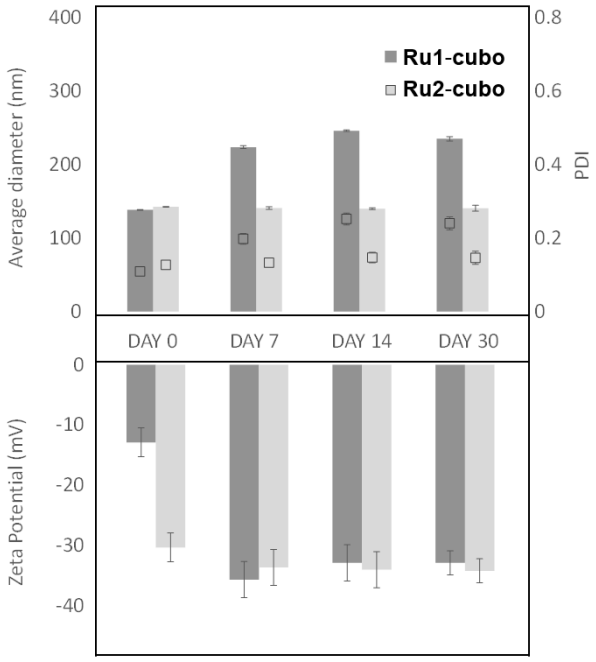

Fig. S16. Average diameter (D, nm), polydispersion index (PDI), zeta potential (ZP, mV) of **Ru1-cubo** and **Ru2-cubo** over 30 days of storage at 25° C.

4.3. Small angle X-ray scattering (SAXS)

SAXS measurements were performed at SAXSLab Sapienza with a Xeuss 2.0 Q-Xoom system (Xenocs SAS, Grenoble, France), equipped with a micro-focus Genix 3D X-ray source with Cu anode (λ = 1.542 Å) and a two-dimensional Pilatus3 R 300K detector which can be placed at variable distance from the sample (Dectris Ltd., Baden, Switzerland). The beam size was defined to be 0.5 mm × 0.5 mm through the two-pinhole collimation system equipped with "*scatterless*" slits. Calibration of the scattering vector q range ($q = 4\pi\sin\theta/\lambda$ with 2θ the scattering angle and λ the photon wavelength), was performed using silver behenate. Measurements with two sample-to-detector distances were performed so that the overall explored q region was 0.004 Å $^{-1}$ < q < 0.6 Å $^{-1}$. The sample was loaded into a vacuum-tight quartz capillary cell and measured in the instrument sample chamber at reduced pressure (~0.2 mbar) within a thermalized holder (21°C). The two-dimensional scattering patterns collected with a total acquisition time of 3.5 hours were subtracted for the "*dark*" counts, and then masked, azimuthally averaged, and normalized for transmitted beam intensity, exposure time and subtended solid angle per pixel, using the FOXTROT software developed at SOLEIL. The one-dimensional intensity *vs.* q profiles were then subtracted for the data of water measured in the same cell and divided by the capillary thickness (0.135 cm) calibrated using water scattering to obtain intensity in absolute scale units (cm^{-1}). The two angular ranges were merged using the SAXS utilities tool.

4.4. Electron microscopy at cryogenic temperature (cryo-TEM)

Cryo-EM micrographs of RPCs embedded into cubosomes were acquired by a ThermoFisher Glacios at 200-keV instrument, equipped with a Falcon III direction electron detector. Holey-carbon R2/2 grids (Quantifoil Micro Tools GmbH) covered by 2 nm film of carbon were prepared. Grid surfaces were treated with plasma cleaning using O_2 for 45 s before applying 3 µL of sample (1 mg/mL in PBS buffer pH 7.4). Grids were blotted in 100% humidity and 10 °C with filter paper and vitrified by rapidly plunging into liquid ethane at -180 °C using a Vitrobot Mark IV (FEI, Hillsboro).

4.5. Cytotoxicity and phototoxicity of Ru(II)-cubosomes formulations

A431 cells were seeded onto 96 well plates at a density of 10^4 cells/well. After 24h incubation, cells were treated with **Ru2-cubo** or E-cubo diluted in complete medium (0.025-0.25 µM **Ru2**, or the corresponding volume for E-Cubo). The experiment and data analysis were carried out as described for the free PS. Each condition was tested in 8 replicates.

4.6. Intracellular ROS production

A431 cells were seeded onto µ-Slide 8 well plates (ibiTreat, Ibidi) at a density of $4x10^4$ cells/well. After 24 h incubation with complete medium, the cells were treated with **Ru2**-**cubo** (100 nM) for 1 hour. After the treatment, cells were washed with PBS and incubated with the intracellular ROS sensor 2,7-dichlorodihydrofluorescein diacetate (DCFH-DA) (2.5 µM in PBS) for 30 minutes. The sensor was removed, and wells were rinsed with PBS before exposure to blue light for 10 minutes or incubation in the dark for the same time. Finally, cells were washed again with PBS, fixed with PFA 4% and stained with Wheat Germ Agglutinin (WGA)-AlexaFluor™ 647-conjugate (ThermoFisher). Cells were observed under a Nikon A1plus confocal laser scanning microscope using a 20x objective. As control, cells without PS were included in the experiment. DCF-positive areas were quantified and normalized to cell-positive areas (quantified from the WGA channel) to obtain the percentage of ROS-producing cells for each treatment. Image analysis was performed with ImageJ.

4.7. Cellular internalization of Ru2 and Ru2-cubo by ICP-AES measurements

A431 cells were seeded onto p100 Petri dishes at a density of $2x10^6$ cells/well and 48 hours later were treated with 0.25 µM **Ru2** or **Ru2-cubo**, equal volume of vehicle or E-cubo, respectively, diluted in growth medium (10% FBS in DMEM) and incubated at 37°C for 1 hour. Then, cells were washed twice in cold PBS, collected by a cell scraper on ice in 1 ml of PBS and centrifuged at 1000xg for 5 minutes. Pellets were maintained at -80°C until the ICP analysis was performed.

A Varian 720-ES axial Inductively Coupled Plasma Atomic Emission Spectrometer (ICP-AES) was used to determine the Ru contents in the samples. Samples were treated with 100 µL of suprapure HNO_3 (obtained by sub-boiling distillation) and, after dissolution, were diluted to a final volume of 5.0 mL with ultrapure water. Measurements were performed in triplicate, and each sample was spiked with 1.0 ppm of Ge, used as an internal standard. The calibration standards were prepared by gravimetric serial dilution from commercial stock standard solutions of Ru at 1000 mg L^{-1} (Honeywell Fluka). For Ru determination, the 267.876 and 245.657 nm wavelengths were used, whereas the line at 209.426 nm was considered for Ge. The operating conditions were optimized to obtain maximum signal intensity, and between each sample, a rinse solution of HNO_3 2% *v*/*v* was used. The results obtained are shown in Fig. S17.

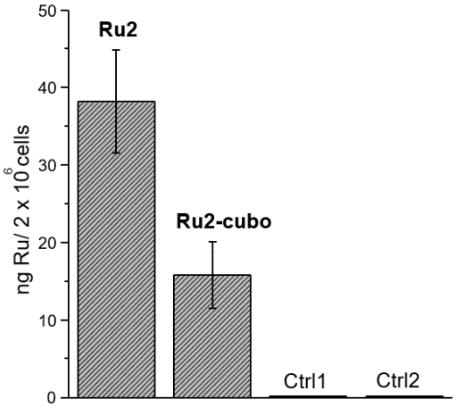

Fig. S17. Cell-uptake as determined by means of ICP-AES analysis for A431 cells incubated for 1 hour with 1 µM **Ru2** or **Ru2**-**cubo** or equal volumes of DMSO (vehicle, Ctrl1) or empty cubosomes (E-cubo, Ctrl2), respectively.

As shown, **Ru2**-**cubo** nanoformulations were effectively internalized by A431 cells, even though in a lesser extent if compared to the free ruthenium complex, in good agreement with the differences also observed between their relative IC_{50} values.

4.8. Cellular internalization of Ru2 and Ru2-cubo by confocal microscopy

A431 cells were seeded onto microscope slides (22x22 mm) at a density of $4x10^5$ cells/well. After 24 h incubation with complete medium (10% FBS in DMEM) cells were treated with 1 µM, **Ru2** or **Ru2**-**cubo**, DMSO (vehicle) or empty cubosomes (E-cubo) for 1 hour at 37°C. Cells were washed with PBS and fixed in 2% paraformaldehyde for 20 minutes, at room temperature. Slides were then incubated with a permeabilization and quenching solution (Triton 0.1% X-100 and ethanolamine (1:165) in PBS). DAPI solution was administered to cell slides to detect nuclei. Slides were mounted by using the Fluoromount Aqueous Mounting

Medium (Sigma-Aldrich, Saint Louis, MA, USA). **Ru2** and **Ru2-cubo** fluorescence were detected using a 405 nm laser diode, acquiring emission in the range of λ 600-630 nm, while DAPI fluorescence was detected at 461 nm. Images were obtained using a Leica SP8 laser-scanning confocal microscope (Leica Microsystems GmbH) using a 63X oil immersion objective. The analysis of **Ru2** and **Ru2-cubo** uptake in A431 epidermoid carcinoma cells showed that the complexes localize to discrete regions of the cell albeit unevenly throughout the cell population (Figure S18). Moreover, the fluorescence distribution of photosensitizer is excluded from the nucleus, demonstrating that despite possible physical interaction between the complexes and DNA, the **Ru2** localization avoid nuclear compartment.

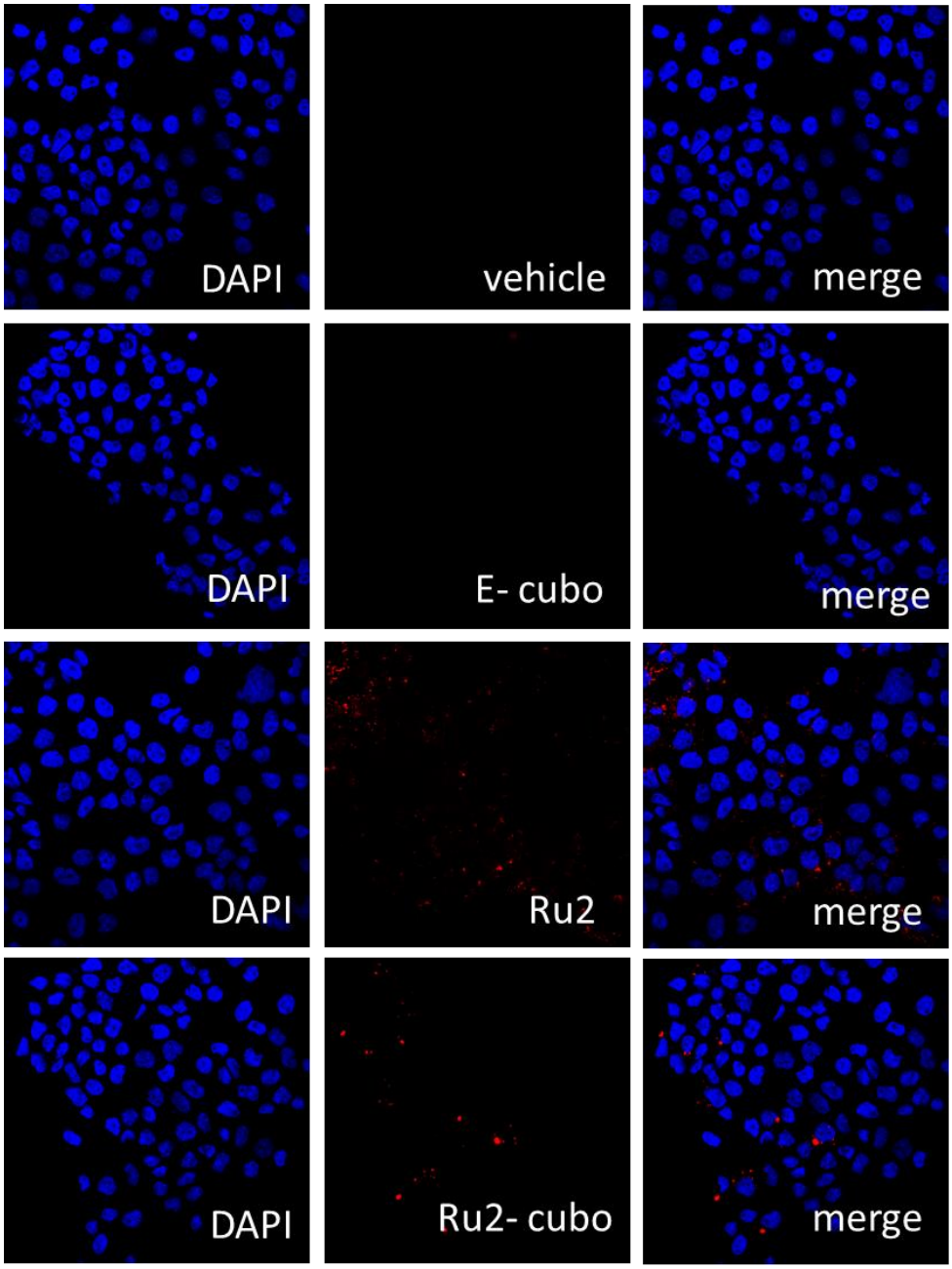

Fig. S18. Internalization of **Ru2** and **Ru2-cubo** in A431 cells by laser-scanning confocal microscopy. A431 cells incubated for 1 hour with 1 μM **Ru2** or **Ru2-cubo** and equal volumes of DMSO (vehicle) or empty cubosomes (E-cubo), respectively. DAPI solution was administered to cell slides to detect nuclei. Images were obtained employing a Leica SP8 laser scanning confocal microscope using a 63X oil immersion objective. DAPI (λ_{exc} = 405 nm, λ_{em} = 461 nm); **Ru2**/**Ru2-cubo** (λ_{exc} = 405 nm, λ_{em} = 600-630 nm).

References

(1) Z. Molphy, A. Prisecaru, C. Slator, N. Barron, M. McCann, J. Colleran, D. Chandran, N. Gathergood and A. Kellett, Copper Phenanthrene Oxidative Chemical Nucleases, *Inorg. Chem.,* 2014, 53 (10), 5392–5404.

(2) P. A. Anderson, G. B. Deacon, K. H. Haarmann, F. Richard Keene, T. J. Meyer, D. A. Reitsma, B. W. Skelton, G. F. Strouse, N. C., Thomas, J. A. Treadway and A. H. White, Designed Synthesis of Mononuclear Tris(Heteroleptic) Ruthenium Complexes Containing Bidentate Polypyridyl Ligands, *Inorg. Chem.,* 1995, 34, 6145-6157.

(3) M. Kubeil, R. R. Vernooij, C. Kubeil, B. R. Wood, B. Graham, H. Stephan and L. Spiccia, Studies of Carbon Monoxide Release from Ruthenium(II) Bipyridine Carbonyl Complexes upon UV-Light Exposure, *Inorg. Chem.,* 2017, 56 (10), 5941–5952.

(4) J. Marmur, A Procedure for the Isolation of Deoxyribonucleic Acid from Micro-Organisms, *J. Mol. Biol.,* 1961, 3, 208-218.

(5) M. E. Reichmann, S. A. Rice, C. A. Thomas and P. Doty, A Further Examination of the Molecular Weight and Size of Desoxypentose Nucleic Acid, *J. Am. Chem. Soc.,* 1954, 76, 3047-3053.

(6) T. Shimidzu, T. Iyoda and K. Izaki, Photoelectrochemical Properties of Bis(2,2'-Bipyridine)(4,4'-Dicarboxy-2,2'-Bipyridine) Ruthenium(II) Chloride, *J. Phys. Chem.,* 1985, 89, 4, 642-645.

(7) K. Kalyanasundaram and MD. K. Nazeeruddin, Protonation Behavior in the Ground and Excited States of Some Os(II) Polypyridyl Complexes, *Inorganica Chim. Acta,* 1990, 171, 213-216.

(8) B. Jing, T. Wu, C. Tian, M. Zhang and T. Shen, pH-Dependent Luminescence of Ruthenium(II) Polypyridine Complexes, *Bull. Chem. Soc. Jpn.,* 2000, 73, 1749–1755.

(9) D. Maggioni, M. Galli, L. D'Alfonso, D. Inverso, M. V. Dozzi, L. Sironi, M. Iannacone, M. Collini, P. Ferruti, E. Ranucci, and G. D'Alfonso, A Luminescent Poly(Amidoamine)-Iridium Complex as a New Singlet-Oxygen Sensitizer for Photodynamic Therapy, *Inorg. Chem.,* 2015, 54 (2), 544–553.

(10) L. Conti, S. Ciambellotti, G. E. Giacomazzo, V. Ghini, L. Cosottini, E. Puliti, M. Severi, E. Fratini, F. Cencetti, P. Bruni, B. Valtancoli, C. Giorgi and P. Turano, Ferritin Nanocomposites for the Selective Delivery of Photosensitizing Ruthenium-Polypyridyl Compounds to Cancer Cell, *Inorg. Chem. Front.* 2022, 9, 1070-1081.

(11) L. Conti, A. Bencini, C. Ferrante, C. Gellini, P. Paoli, M. Parri, G. Pietraperzia, B. Valtancoli, and C. Giorgi, Highly Charged Ruthenium(II) Polypyridyl Complexes as Effective Photosensitizer in Photodynamic Therapy, *Chem. - A Eur. J.,* 2019, 25, 10606-10615.

(12) M. Sirajuddin, S. Ali and A. Badshah, Drug-DNA Interactions and Their Study by UV-Visible, Fluorescence Spectroscopies and Cyclic Voltametry, *Journal of Photochemistry and Photobiology B: Biology*., 2013, 124, 1-19..

(13) L. Conti, A. Mengoni, G. E. Giacomazzo, L. Mari, M. Perfetti, C. Fagorzi, L. Sorace, B. Valtancoli and C. Giorgi, Exploring the Potential of Highly Charged Ru(II)- and Heteronuclear Ru(II)/Cu(II)-Polypyridyl Complexes as Antimicrobial Agents, *J. Inorg. Biochem.,* 2021, 220, 111467.